

Low-field magnetization studies in the reentrant superconductor $\text{ErRh}_{1.1}\text{Sn}_{3.6}$

K. Andres, J. P. Remeika, G. P. Espinosa, and A. S. Cooper

Bell Laboratories, Murray Hill, New Jersey 07974

(Received 15 August 1980)

Absolute static magnetization measurements in fields as low as 0.1 Oe in a single crystal of $\text{ErRh}_{1.1}\text{Sn}_{3.6}$ show a clear Meissner effect at the superconducting transition. In the superconducting state, the magnetization shows reversible type-II behavior above a field of 6 Oe, and a thermodynamic critical field $H_0 = 20 \pm 5$ Oe can be deduced from the data. The previously reported reduction in H_{c2} upon cooling towards the ferromagnetic Curie temperature ($T_C = 0.46$ K) can be explained entirely as being due to the increasing paramagnetic induction in the sample. A search for a coexistence region of superconductivity and ferromagnetism below T_C indicates that such a region must be smaller than 0.03 K.

I. INTRODUCTION

In reentrant superconductors, where superconductivity is destroyed upon lowering the temperature, owing to the onset of long-range magnetic order, the detailed behavior around the magnetic ordering temperature and the question of a coexistence region of magnetic order and superconductivity are of central interest. In the case of ErRh_4B_4 , where superconductivity sets in at 8.5 K and is destroyed by ferromagnetic order below 0.93 K, evidence for a coexistence region has come from several experiments.^{1,2} In some of those, however, it is doubtful whether coexistence is a truly microscopic property or whether it can in part be explained by inhomogeneities in the samples, particularly since one has not been able to prepare ErRh_4B_4 in single-crystal form.

It is therefore of special interest that the recently discovered reentrant superconductor $\text{ErRh}_{1.1}\text{Sn}_{3.6}$ [$T_c = 1.36$ K, $T_C = 0.46$ K (Ref. 3-6)] can be prepared in single-crystal form, in which one would expect a much improved sample homogeneity. The crystals were prepared by reacting Er and Rh with a surplus of Sn in a sealed evacuated quartz tube at 1050 °C for 2 h. The melt was then slow cooled to 575 °C and removed from the furnace.⁷ The crystals show large natural growth faces, and have a tetragonal crystal structure with lattice parameters of $a_0 = 13.732$ Å and $c_0 = 27.418$ Å.⁸⁻¹⁰ In the original work, this compound is designated phase II.

We have carried out careful static magnetization measurements in low magnetic fields on a small ($m = 16.7$ mg) single-crystal piece of $\text{ErRh}_{1.1}\text{Sn}_{3.6}$ in order to investigate its paramagnetic and superconducting properties (such as the Meissner effect and the lower and upper critical fields), to search for a coexistence region, and to determine some properties

of the ferromagnetic state. Some measurements have also been done on a sample of ErRh_4B_4 for comparison.

II. APPARATUS

A moving-coil magnetometer with superconducting field and pickup coils, mounted in a dilution refrigerator, was used for the measurements.¹¹ It is designed for high sensitivity in low magnetic fields ($H \leq 100$ Oe) and uses a superconducting-quantum-interference-device (SQUID) sensor as a detector. Two samples can be mounted (with Apiezon grease) to a copper coldfinger which is thermally anchored to the mixing chamber and passes through the center of the coil system. The latter can move vertically on rollers inside a frame and is suspended by two silk threads from a motor mechanism mounted on top of the cryostat. It is thermally anchored to the first heat exchanger in the refrigerator and cools to about 0.4 K. By means of the remote-controlled motor mechanism, it can be moved from a neutral position to an upper position, where the upper sample enters the upper coil, and to a lower position, where the lower sample enters the lower coil. The corresponding flux changes are observed with a SHE model 330 SQUID system either in an analog mode (up to 500 flux quanta) or in a digital mode (up to 10^5 flux quanta). Whenever the measuring field is changed, a superconducting indium shield around the astatic pair of pickup coils has to be heated briefly to freeze in the new field. This procedure leaves the temperature of the coldfinger (which is monitored by calibrated carbon resistors) unchanged except in the region below 100 mK, where a small transient warm-up occurs. The intensity of the residual magnetic

field in the laboratory (~ 0.4 Oe) is reduced to about 1% of this value by a large Permendur shield around the cryostat.

III. MEISSNER EFFECT AND FLUX FREEZING

As the lower critical field H_{c1} of $\text{ErRh}_{1.1}\text{Sn}_{3.6}$ is about 1 Oe (see below), the Meissner effect was measured in a field as low as 0.1 Oe. Figure 1 shows the cooling—and subsequent warming curve in this fixed field. After the paramagnetic rise to $T_C = 1.36$ K, flux is expelled down to 1.14 K, where surface supercurrents lock in the flux and keep it constant upon further cooling. At 1.14 K, the Meissner effect is given by the fraction f of the field-free (superconducting) volume, which is given by

$$f = (m_p - m) / (m_p - m_{s,0}) = 0.22, \quad (1)$$

where m is the observed magnetization at 1.14 K, m_p the paramagnetic value in the absence of superconductivity, and $m_{s,0}$ the fully superconducting signal. This latter signal can be obtained for example, by cooling the sample in zero field to 0.66 K and then applying a field of 0.1 Oe. [See Fig. 1. The ratio of $f = a/b$ of Eq. (1) is also indicated in the figure.] The pure paramagnetic signal m_p (dashed line) is obtained by scaling down the magnetization data in $H = 20$ Oe (Fig. 4, see below). The sample had the approximate shape of a rod with a length to thickness ratio of about 4. Demagnetization effects are thus relatively small (the demagnetization factor is 0.95) and have been neglected for determining f . Ideal Meissner effects ($f = 1$) are only observed in carefully annealed high-purity superconductors. For com-

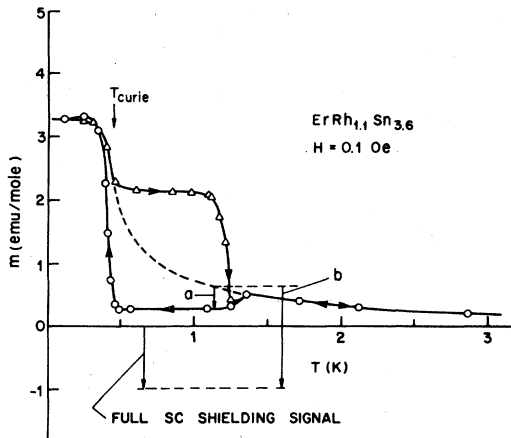


FIG. 1. Observed magnetization in an $\text{ErRh}_{1.1}\text{Sn}_{3.6}$ single crystal upon cooling (\circ) and subsequent warming (Δ) in a constant applied field of 0.1 Oe. The full SC shielding signal is obtained by cooling in $H = 0$ to 0.65 K and then applying $H = 0.1$ Oe.

parison, small (unannealed) chips cut from a high-purity aluminum bar showed only a 60% Meissner effect. The observed value of 22% for $\text{ErRh}_{1.1}\text{Sn}_{3.6}$ thus indicates that superconductivity occurs in the whole crystal and not just in filaments.

Below the ferromagnetic transition at 0.46 K, superconductivity disappears and a ferromagnetic signal is observed. Due to the small applied field, the latter is only a small fraction (5.3×10^{-3}) of the saturation magnetization. When warming from below T_C , one first follows the dashed line, which is scaled down from the 20-Oe data, until right at T_C supercurrents again begin to lock any further decrease in magnetization. One then has to warm up to 1.1 K until the supercurrents begin to die out again and one eventually returns to the normal-state values above T_C .

IV. MAGNETIZATION CURVE IN THE SUPERCONDUCTING STATE

In an attempt to determine the superconducting (diamagnetic) magnetization in the sample, it was cooled in zero field into the superconducting region and the total magnetization measured at constant temperature in increasing applied fields. The low-field region at three temperatures is shown in Fig. 2(a), where it can be seen that the sample is perfectly diamagnetic only in fields up to about 1 Oe. At 0.725 K, flux penetration starts at 1.5 Oe and the net signal becomes paramagnetic above 3 Oe. In the higher field range, shown in Fig. 2(b), we can detect the presence of a diamagnetic contribution up to about 80 Oe. Upon reducing the field again, the magnetization is reversible down to 6 Oe, where flux trapping begins. Above 6 Oe, thus, the sample exhibits reversible type-II behavior. Although we do not know the microscopic distribution of the magnetization in the sample, we can still extract the net amount m_s of superconducting diamagnetism from the equation

$$m = m_p + m_s = \chi_p^* H y + \chi_s^* H (1 - y),$$

with

$$\chi_p^* = \frac{\chi_p}{1 + N_p \chi_p}, \quad \chi_s^* = \frac{-1/4\pi}{1 - N_s/4\pi}. \quad (2)$$

Here χ_p^* and χ_s^* are the apparent volume susceptibilities in the paramagnetic (field penetrated) and in the superconducting (field excluding) regions in the sample, and y is the net fraction of field penetration. The demagnetization factors N_p and N_s are only well defined in the purely superconducting ($y = 0$) and purely paramagnetic ($y = 1$) states, where they are $N_p = N_s = 0.95$. For simplicity, we use $N_s = 0$ for $H > 2$ Oe (where field penetration has already started) and $N_p = 0.95$ for all fields. This may underesti-

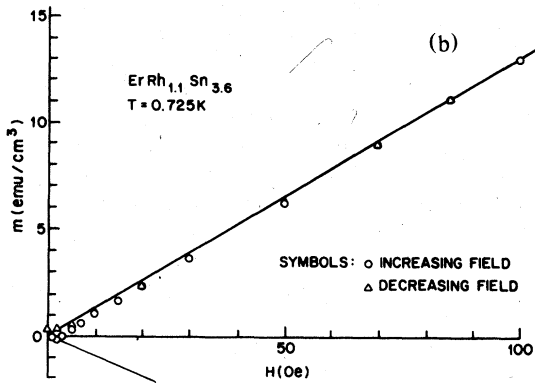
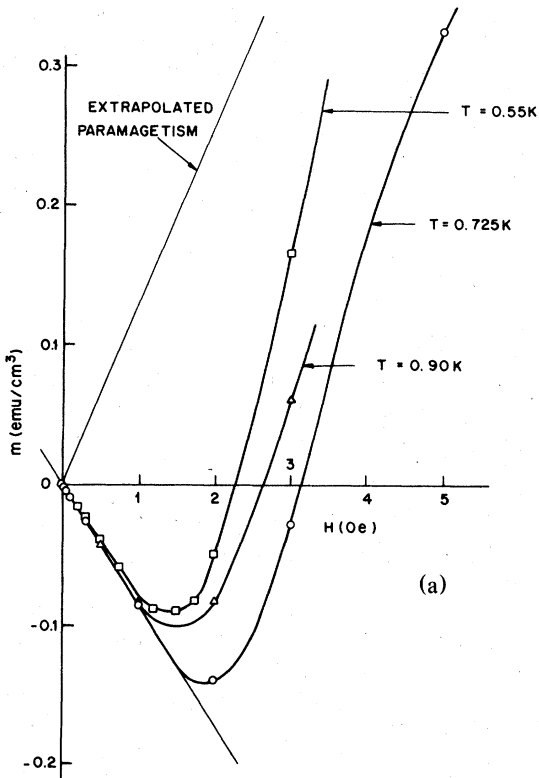


FIG. 2. (a) and (b): Observed magnetization with increasing applied field after cooling in $H = 0$ to various temperatures.

mate m_s somewhat in the low-field region. From Eq. (2) we obtain

$$y = \frac{m - \chi_s^* H}{\chi_p^* H - \chi_s^* H} \quad (3)$$

and hence

$$m_s = \frac{-1/4\pi}{1 - N_s/4\pi} (1 - y) H = \frac{\chi_p^* H - m}{\chi_p^*/\chi_s^* - 1} \quad (4)$$

A plot of m_s vs H is given in Fig. 3, where the large error bars at higher fields stem from the fact that the small diamagnetic signals are superimposed on a large paramagnetic background. Extrapolating the reversible type-II behavior through the irreversible region below 6 Oe (dashed line in the insert of Fig. 3), we can determine the lower critical field H_{c1} . For H_{c2} we can only give a lower limit. We obtain at $T = 0.725$ K:

$$H_{c1} = 1.3 \text{ Oe}, \quad H_{c2} \geq 80 \text{ Oe} \quad (5)$$

The estimated values for H_{c1} at 0.55 and 0.90 K are 0.5 and 1.0 Oe, respectively.

Using Fig. 3, we can also determine approximately the thermodynamic critical field from the area under the magnetization curve:

$$-\frac{1}{4\pi} \frac{H_c^2}{2} = \int m_s dH \quad (6)$$

We obtain $H_c = 13.5$ Oe at 0.725 K, which would yield

$$H_0 = H_c [1 - (T/T_c)^2]^{-1} = 19.5 \pm 5 \text{ Oe} \quad (7)$$

This is an unusually low value for a superconducting transition temperature of 1.36 K and points to gapless superconductivity in $\text{ErRh}_{1.1}\text{Sn}_{3.6}$.

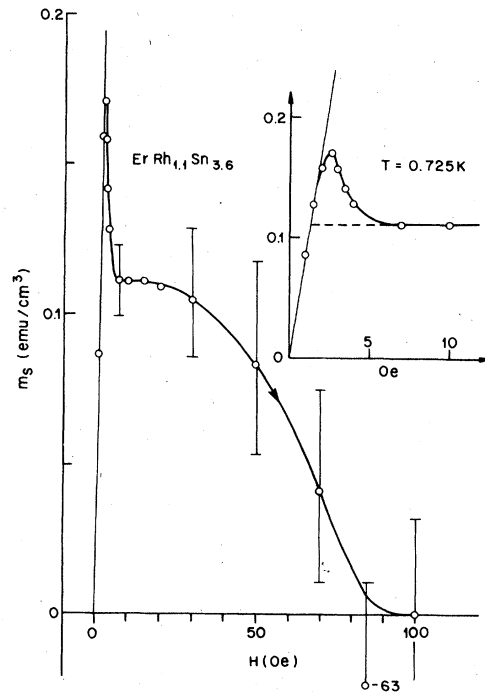


FIG. 3. Superconducting (diamagnetic) magnetization m_s , extracted from the data of Fig. 2 (see text), plotted vs applied field H .

V. SUSCEPTIBILITY IN THE PARAMAGNETIC STATE

The superconducting shielding signals provide a convenient absolute calibration for paramagnetic susceptibility measurements (χ_p). Due to the low critical fields and the large paramagnetic susceptibilities, χ_p is only slightly reduced by superconductivity in higher fields. This is shown by the magnetization data in $H = 20$ Oe in Fig. 4. Using the data of Fig. 2(b), the estimated value of $m_p = \chi_p \dot{H}$ (in the absence of superconductivity) is shown dashed. From the inflection point in m_p vs T we deduce a ferromagnetic transition temperature of 0.46 ± 0.03 K. A plot of χ_p^{-1} vs T , corrected for demagnetization effects, is also given in Fig. 4. We see that χ_p closely follows a Curie-Weiss law of the form

$$\chi_p = C / (T - \Theta) \quad (8)$$

with

$$C = 7.04 \text{ emu K/mole}, \quad \Theta = 0.17 \text{ K}.$$

For the conversion from volume to molar susceptibilities, a molar volume of 77.77 cm^3 has been used.⁶ For comparison, the Curie constant for free Er^{3+} ions equals 11.48 emu K/mole . Since specific-heat and entropy measurements,⁶ are consistent with a doublet ground state for the Er^{3+} ions, the theoretical Curie constant would be

$$C = \frac{L (g^* \mu_B)^2 3}{12k} \quad (9)$$

where L is Avogadro's number, g^* is the effective g factor of the doublet state, and K is Boltzmann's constant. From Eqs. (8) and (9) we then deduce an effective moment for the ground-state doublet of

$$\mu_{\text{eff}} = g^* \mu_B = 8.66 \mu_B \quad (10)$$

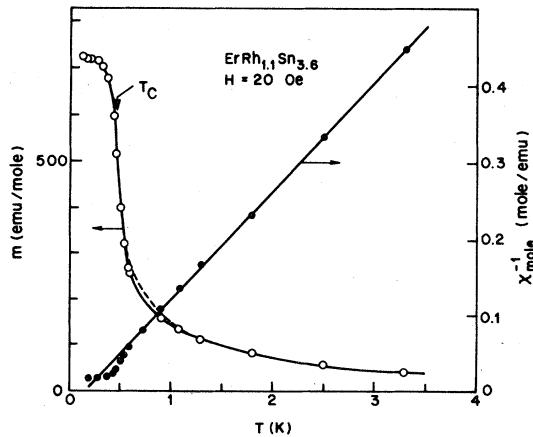


FIG. 4. Observed magnetization in an applied field of 20 Oe. The dashed line indicates the pure paramagnetic values (with the diamagnetic contribution from superconductivity subtracted), which have been used in the plot of χ^{-1} vs T (right-hand scale).

This suggests that the doublet ground state is close to being a $\pm J$ state, which, with $J = \frac{15}{2}$ and $g_J = \frac{6}{5}$ would have a moment of

$$\mu = J g_J \mu_B = 9 \mu_B \quad (11)$$

VI. CALCULATION OF THE "INTERNAL" UPPER CRITICAL FIELD H_{c2}^*

The previously observed⁶ values of H_{c2} are somewhat larger than our magnetization measurements suggest. They increase below T_c to a maximum of 110 Oe at 0.9 K and then decrease again to zero upon approaching the ferromagnetic transition. Since for fields close to H_{c2} one has nearly complete and uniform flux penetration, it is of interest to determine how much of the reentrant decrease of H_{c2} is due to the growing paramagnetic induction in the sample. Thus we can calculate an effective critical field H_{c2}^* which is equal to the total induction in the sample at H_{c2} :

$$H_{c2}^* = B = H_{c2} (1 + 4\pi \chi_p^*) \quad (12)$$

Here χ_p^* is the observed paramagnetic susceptibility shown in Fig. 4. If we adjust the H_{c2} data of Ref. 6 to the transition temperatures of our sample, we obtain the H_{c2}^* -curve shown in Fig. 5. As can be seen, the anomalous decrease towards lower temperatures has almost vanished, which confirms that superconductivity in $\text{ErRh}_{1.1}\text{Sn}_{3.6}$ is destroyed mainly by the internal molecular (dipolar) field due to the Er^{3+} ions, rather than by the increased pair breaking effect due to the net spin polarization. This is in agreement with the fact that the Er^{3+} moment is mostly of orbital origin [Eqs. (10) and (11)] and might at first suggest that in zero applied field there is a coexistence region which extends to that temperature at which the induction in the ferromagnetic domains has reached 300 G (see Fig. 5). For ferromagnetic inductions less than but still close to 300 G, the domain magnetization in the dense vortex structure is still nearly uniform and one could imagine that ferromagnetism might therefore coexist with superconductivity in a narrow temperature range. For smaller domain magnetizations (i.e., closer to the Curie temperature), the magnetization would become spatially nonuniform due to the less dense vortex structure in the type-II state and would no longer be compatible with a uniform ferromagnetic state. Blount and Varma¹² have shown theoretically that a uniform ($q = 0$) ferromagnetic state cannot coexist with superconductivity. These authors also argue that a state of spontaneous vortex structure would not be stable, since the London penetration depth λ , which applies for external applied fields, has to be replaced by an effective penetration depth λ' when the induction is due to spontaneous magnetization. It turns out that

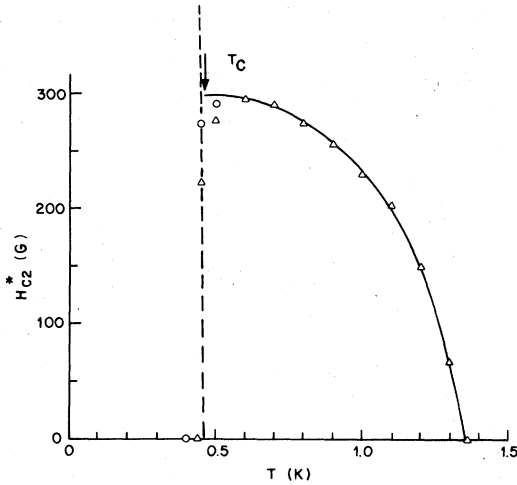


FIG. 5. Plot of the effective upper critical field H_{c2}^* vs temperature (see text). Also shown (dashed) is the estimated domain induction in the ferromagnetic state.

$\lambda' = (\lambda\delta)^{1/2}$ (δ the magnetic stiffness parameter) is much smaller than λ . The condition $\lambda' \gg \xi$ (ξ the superconducting coherence length) for type-II superconductivity is therefore no longer fulfilled and the material behaves as a type-I superconductor. The theoretical predictions^{12,13} then, are that below T_C , superconductivity first suppresses ferromagnetism (in zero applied field), then a second-order transition to a superconducting state with a spiral type (finite q) long-range magnetic order may occur, and, at still lower temperatures, a first-order transition to the uniform ferromagnetic and nonsuperconducting state takes place. If at that transition the ferromagnetic induction is 300 G, as our data in Fig. 5 suggest, we can estimate how much below the Curie temperature it would be. According to Eq. (10), the saturation induction at zero degrees is

$$B_s = 4\pi L \mu_{\text{eff}} / V_m = 7815 \text{ G} . \quad (13)$$

Describing the domain magnetization by

$$m/M_s = 1 - (T/T_C)^{3/2} , \quad (14)$$

we would calculate that the transition occurs 11 mK below the Curie temperature. The temperature region for any possible coexistence phenomena is thus very small.

VII. SEARCH FOR COEXISTENCE AND SOME PROPERTIES OF THE FERROMAGNETIC STATE

Some peculiar behavior of ferromagnetic remanence is observed after cooling the sample in zero field, then applying 100 Oe and removing it again. If this is done at 0.1 K, we observe a small remanence

(of order 10^{-3} of the saturation magnetization), which, upon heating, disappears very quickly below the Curie temperature. When it is done at 0.25 K, the remanence is larger and now disappears completely only when warming up to the Curie temperature. This behavior, which is indicated in Fig. 6, might mean either that there are different types of domain walls, some of which move more easily at low temperatures than others, or that one can initiate magnetization changes within the domains (without moving domain walls). This latter possibility might arise from an inherent disorder among the erbium ions and is so far not inconsistent with neutron scattering and x-ray results.^{3,10}

Closely below the ordering temperature of 0.46 K, magnetization measurements in $H = 0.1$ Oe at 0.435 K reveal no sign any more of superconducting shielding currents. Another test for possible coexistence of superconductivity and ferromagnetism was carried out as follows: In the superconducting state, an amount of positive flux was frozen into the sample by applying a field of 30 Oe and removing it again (i.e., some flux was retained by supercurrents). If a coexistence region exists, one would expect to end up with a small amount of ferromagnetic remanence after cooling below T_C . No such remanence could be detected in our sample of $\text{ErRh}_{1.1}\text{Sn}_{3.6}$, i.e., all supercurrents seemed to have ceased before the onset of ferromagnetism. This is shown by the data in Fig. 7,

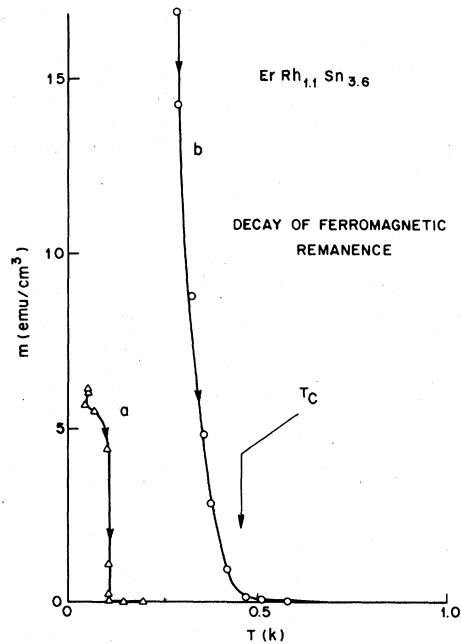


FIG. 6. Observed decay of ferromagnetic remanence in $\text{ErRh}_{1.1}\text{Sn}_{3.6}$ with increasing temperature after applying and removing $H = 100$ Oe at $T = 0.1$ and 0.25 K.

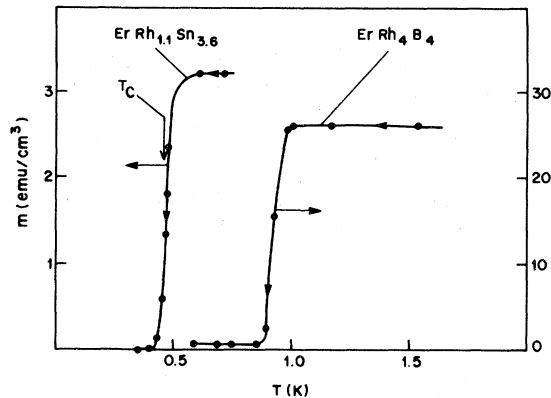


FIG. 7. Observed reduction of frozen-in magnetization when cooling through the Curie temperature (see text).

from which we would deduce a transition to the ferromagnetic state around 0.43 K. These data as well as those of Fig. 1 indicate that in low applied fields, the transition to the ferromagnetic state occurs at slightly lower temperatures than in higher applied fields. [From our measurements in $H = 20$ Oe (Fig. 4), where the flux penetration close to T_C must be fairly uniform, we deduce $T_C = 0.46$ K from the inflection point of the magnetization curve.] Although

this shift from 0.46 to 0.43 K is somewhat uncertain because of the finite width of the transitions (it is in fact larger than the estimated maximum value of 11 mK mentioned above), the data indicate that it may indeed exist, as theoretically predicted.^{12,13} A similar experiment in a polycrystalline sample of ErRh_4B_4 , on the other hand, did reveal a small amount of remanence, as shown in Fig. 7. In this latter material, the transition to the ferromagnetic state could occur about 0.1 K below the Curie temperature, because the internal critical field H_{c2}^* [Eq. (12)] necessary for the destruction of superconductivity is roughly ten times larger. While this experiment shows that there might be a small coexistence region in ErRh_4B_4 in this temperature interval, it is impossible to rule out that the observed remanence might also have been caused by inhomogeneities in the sample.

ACKNOWLEDGMENTS

We would like to thank C. M. Varma for illuminating discussions and D. B. McWhan and J. M. Rowell for their interest and encouragement during this work. We also thank H. Barz for checking T_C on several crystals.

¹D. E. Moncton, *J. Appl. Phys.* **50**, 1880 (1979).

²H. R. Ott, W. A. Fertig, D. C. Johnston, M. B. Maple, and B. T. Matthias, *J. Low Temp. Phys.* **33**, 159 (1978).

³J. P. Remeika, G. P. Espinosa, A. S. Cooper, H. Barz, and J. M. Rowell, *Bull. Am. Phys. Soc.* **25**, 232 (1980).

⁴J. M. Vandenberg, J. P. Remeika, A. S. Cooper, G. P. Espinosa, and H. Barz, *Bull. Am. Phys. Soc.* **25**, 232 (1980).

⁵Z. Fisk, H. C. Hamaker, M. B. Maple, L. D. Woolf, and J. P. Remeika, *Bull. Am. Phys. Soc.* **25**, 232 (1980).

⁶J. P. Remeika, G. P. Espinosa, A. S. Cooper, H. Barz, J. M. Rowell, D. B. McWhan, J. M. Vandenberg, D. E. Moncton, Z. Fisk, L. D. Woolf, H. C. Hamaker, M. B. Maple, G. Shirane, and W. Thomlinson, *Solid State Commun.* **34**, 923 (1980).

⁷G. P. Espinosa, *Mater. Res. Bull.* **15**, 791 (1980).

⁸A. S. Cooper, *Mater. Res. Bull.* **15**, 799 (1980).

⁹J. L. Hodeau, J. Chenavas, M. Marezio, and J. P. Remeika, *Solid State Commun.* (in press).

¹⁰J. Chenavas, J. L. Hodeau, A. Collomb, M. Marezio, J. P. Remeika, J. M. Vandenberg, in *Proceedings of the International Conference on Ternary Superconductors*, Lake Geneva, Wisconsin, September 1980 (unpublished).

¹¹K. Andres *et al.*, *Phys. Rev. A* (in press).

¹²E. I. Blount and C. M. Varma, *Phys. Rev. Lett.* **42**, 1079 (1979).

¹³C. M. Varma, in *Proceedings of the Third Conference on Superconductivity in d- and f-Band Metals, La Jolla, June 1979*, edited by H. Suhl and D. Maple (Academic, New York, 1980).